Modulating the Optical Properties of Citrazinic Acid through the Monomer-To-dimer Transformation

Modulating the Optical Properties of Citrazinic Acid through the Monomer-to-Dimer Transformation

Stefania Mura,[†] Luigi Stagi,[†] Luca Malfatti,[†] Carlo Maria Carbonaro,[‡] Robert Ludmerczkĭ,[†] and Plinio Innocenzi*[,†]

[†]
Department of Chemistry and Pharmacy, Laboratory of Materials Science and Nanotechnology, CR-INSTM, Via Vienna 2, 07100
Sassari, Italy

[‡]Department of Physics, University of Cagliari, sp n°8, km 0.700, 09042 Monserrato, Italy

* Supporting Information

ABSTRACT: Understanding the luminescence of carbon dots is a highly challenging task because of the complex reactions involved in the synthesis process. Several by-products form at different reaction stages and become possible sources of emission. Citrazinic acid and its derivatives, in particular, have been identified as intermediates that give rise to blue fluorescence. Full comprehension of the optical properties of citrazinic acid itself is, however, still lacking. In particular, citrazinic acid has the property of forming different tautomers and aggregates such as dimers. However, the nature of these chemical species and the correlation with their relative optical properties have been only partially explored. In the present work, we have used a combination of spectroscopic techniques, UV−visible and fluorescence spectroscopy, time-resolved photoluminescence and computational simulation, to study the different species which citrazinic acid forms in water as a function of CZA molarity. A monomer-todimer transformation and a hypsochromic shift are observed with concentration. The monomer is in the keto structure and does not form other tautomers while the dimers are fluorescent J-type aggregates. The formation of aggregates strongly modulates the optical properties of citrazinic acid.

INTRODUCTION

The controlled pyrolysis of organic precursors, such as citric acid, is one of the most common syntheses to prepare fluorescent carbon dots. This reaction, however, produces several intermediates, which are also fluorescent and the whole control of the process has revealed to be a challenging task. Even the formation of carbon dots by hydrothermal process, employing as precursor only citric acid, has revealed the presence of several fluorescent intermediate species.[1] The importance of the role played by the intermediate by-products of the reaction has emerged as a critical issue in the synthesis of fluorescent carbon dots.[2] To obtain carbon dots, high temperatures of carbonization are employed, generally at least 200 °C; at this temperature, molecular fluorophores can be present and be responsible for the observed emission. This awareness has highlighted the need for studying the details of the reactions and properties of intermediate compounds. The reaction of citric acid with amines, in particular, gives highly fluorescent species and blue-emitting carbon dots.[3−5] Citric acid reacts with ammonia or urea and forms citrazinic acid as a fluorescent intermediate; citrazinic acid derivatives also form upon reaction with other precursors bearing amines. Hydrothermal synthesis of carbon dots using citric acid and ethylenediamine as precursors gives a fluorescent citrazinic derivative with a very high quantum yield.[6]

The role played by the citrazinic derivatives in nitrogendoped carbon dots has been the subject of systematic investigations.[7] It has clearly emerged that the contribution of such species to the blue emission cannot be neglected and that the general model to explain the origin of fluorescence in carbon dots should take into account the formation of fluorescent derivatives.[8]

Understanding the properties of the intermediate such as citrazinic acid is, therefore, a mandatory step for achieving an efficient control of carbon dots synthesis. Quite surprisingly, there are no recent studies on citrazinic acid, in particular, focused on the optical properties.[9,10]

Citrazinic acid (2,6-dihydroxyisonicotinic acid) and its derivatives have been observed to form fluorescent intermediates and therefore are of paramount importance to control the emission of CDs. CZA is a heterocyclic compound formed by a dihydroxy-pyridine ring with a carboxylic acid group substitution; it is fluorescent with emission in the blue range and forms tautomers as a function of pH.[11] A detailed study of its properties related to its concentration in solution is still lacking, but it is a mandatory step to understand the species formed during aggregation and how the fluorescence is affected by the different aggregation states. This is the subject of the present article.

EXPERIMENTAL AND THEORETICAL METHODS

Citrazinic acid (purity 97%, Sigma-Aldrich) and water (milliQ) were used as received without further purification. Different solutions of citrazinic acid (CZA) in water were prepared with concentrations of 10, 30, 40, 50, 70, 90, and 110 mg L^{-1}.

Characterization. UV−vis measurements of CZA solubilized in water were carried out in absorbance, using a Nicolet Evolution 300 spectrophotometer from 200 to 600 nm. The data were analyzed with ORIGIN Pro 8 software.

Three-dimensional fluorescence mapping (excitation−intensity−emission) of the CZA solutions in water was performed using a Horiba Jobin Yvon FluoroMax-3 spectrofluorometer and a 450 W xenon lamp as the excitation source. The maps were collected with an excitation range of 200−700 nm and an emission range of 200−700 nm with a 1 nm slit for excitation and emission.

Time-resolved fluorescence (TRF) measurements in the nanosecond time domain were performed using the TBX picosecond detection module connected to a Nanolog spectrometer (Horiba Jobin Yvon Inc.). The samples were excited with a 340 nm LED source (1 MHz repetition rate and pulse width <1.2 ns). Data were collected immediately after laser decay. The acquisition time resolution is 0.11 ns.

Computational Details. All of the calculations were carried out using Gaussian 16 code.[12] The energy calculations of the optimized structures were performed within density functional theory (DFT) with Becke's three parameters and the Lee−Yang−Parr's nonlocal correlation functional [13-15] (B3LYP). The basis sets for C, N, O, and H were 6-311++G(d,p), while the electronic excitation energies were calculated on the basis of the TD-DFT method. Analysis of frequencies confirms that optimized structures are at a minimum of potential surface, and no imaginary frequencies were obtained. The calculations were performed in the polarizable continuum model (PCM) using the integral equation formalism variant (IEFPCM).[16] The calculations were performed using both water and vacuum as the medium. GaussView 6 were used to interpret the computed data.[17]

RESULTS AND DISCUSSION

Citrazinic acid is characterized, thanks to the presence of conjugated bonds in the pyridine ring, by emission in the blue zone of the spectrum. CZA can be present in solution in different forms, such as tautomers or as aggregates. To study the formation of these species and their optical response, we have used aqueous solutions of CZA at increasing concentrations. The formation of the different species has been studied by combining several spectroscopic techniques and theoretical calculations.

Assessment of the CZA Species in Water by UV−Vis Spectroscopy. Figure 1 shows the UV−vis absorption spectra of citrazinic acid in water at different concentrations from 10 up to 110 mg L^{-1}. The spectra are characterized by a strong absorption in the UV region with a band at around 235 nm, a valley at 276 nm, and another absorption band peaking at 344 nm (10 mg L^{-1}). The UV absorption band at around 235 nm is attributed to π−π* transitions, due to conjugated π electrons in aromatic rings, while the band peaking at around 344 nm is assigned to n−π* transitions.

The n−π* transition absorption band increases in intensity and shifts to shorter wavelengths (blue shift) as a function of citrazinic acid concentration (Figure 2a). The increase in

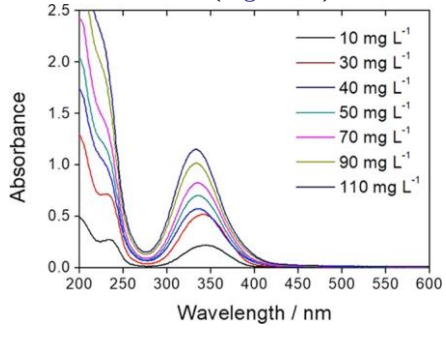

Figure 1. UV−vis absorption spectra of aqueous solutions of citrazinic acid at increasing concentrations from 10 up to 110 mg L^{-1}.

absorbance and the blue shift follow a linear trend with the concentration. The hypsochromic shift is attributed to the change in polarity produced by higher concentrations of CZA. The higher is the content of CZA in the solutions, higher will be the polarity. A comparison with a solution of CZA in ethanol, which has a lower polarity with respect to water, supports this explanation of the cause of the blue shift (Figure S1). We have compared the UV−vis spectra of CZA in ethanol with those in water, and a hypsochromic shift of about 15 nm has been observed. The higher polarity of the water stabilizes more the ground state than the excited one, and this is reflected in an increase of the energy gap between the excited and the ground state.

A comparison of the UV−vis normalized spectra at different CZA concentrations shows the presence of an isosbestic point at 377 nm, which indicates the formation of two species in equilibrium (Figure 2b). At higher concentrations, CZA dimers form and coexist with the monomers. The linear increase in absorbance demonstrates that CZA, in the experimental range of concentrations, does not form large aggregates that could precipitate. The species in solution would be monomers and dimers. To follow in detail the formation of dimers, we have deconvoluted the absorption spectra using two Gaussian components. Figure 3a shows the best fitting to CZA absorption spectrum at the concentration of 110 mg L^{-1}. The full set of deconvoluted spectra can be found in Figure S2. The absorption band is formed by two components, one of higher intensity, peaking at 330 nm and assigned to the monomeric form, and a second one at 370 nm, attributed to the formation of dimers.

The curve fits show that at the lowest concentration of CZA in water, 10 mg L^{-1}, only monomers are present. The formation of dimers (Figure 3b) begins at higher concentrations from 30 mg L^{-1}. The best fit of the absorption band is obtained with two Gaussian components. At 50 mg L^{-1}, the dimer content is doubled in comparison with the 30 mg L^{-1} solution.

Quantum Chemistry Calculations. Another issue to be addressed is the possible formation of CZA tautomers and their role in the dimerization. We have performed theoretical calculations to separate the possible contributions from different tautomers. The ground state geometries of the monomer forms of citrazinic acid have been optimized using density functional theory (DFT). Two possible tautomeric configurations of the monomers, in the forms of imine and keto, have been used[18] (Scheme 1).

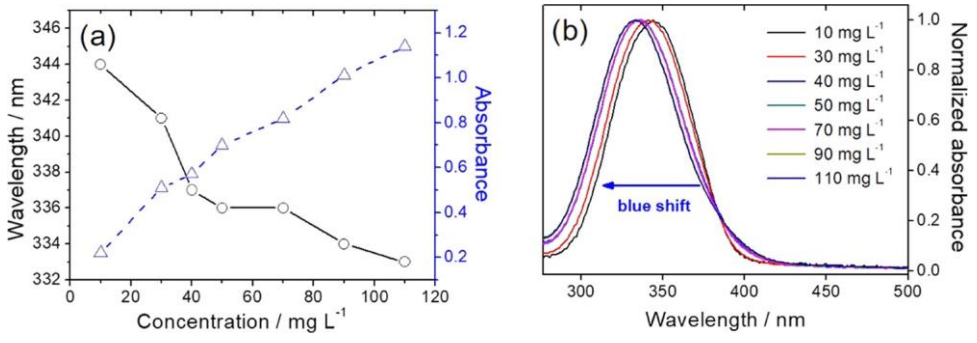

Figure 2. (a) Change of the absorption maxima intensity and wavelength as a function of citrazinic acid concentration. The lines are a guide for eyes. (b) Normalized absorption spectra of the 344 nm absorption band.

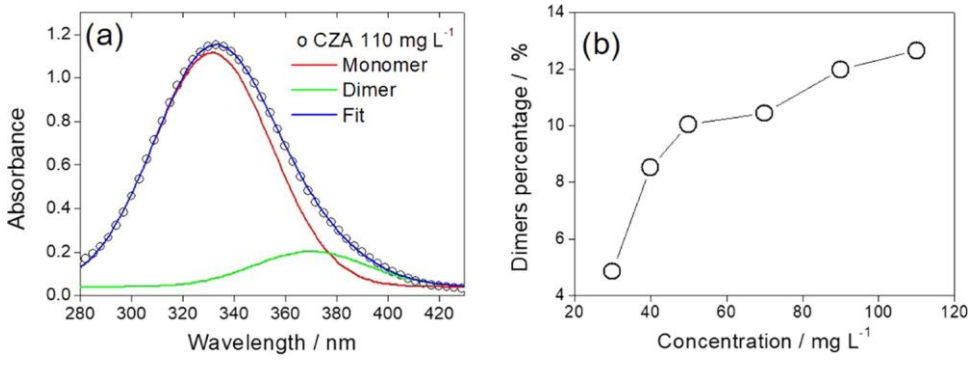

Figure 3. (a) Curve fit of the 330 nm absorption band of CZA at a concentration of 110 mg L^{-1} in water. (b) The change of dimer content as a function of concentration calculated as the ratio between 370 nm band and the total absorption band areas obtained from the deconvolution. The line is a guide for eyes.

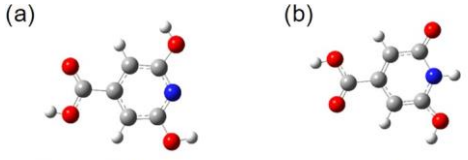

Scheme 1. CZA Tautomer Structure: (a) IMINE and (b) KETO Forms

experimental ones, in particular, the UV−vis absorption spectra, suggest that the only monomeric species of citrazinic acid in solution is the keto one. Moreover, the self-consistent field (SCF) energy values reported in Table S1 show that the keto configuration is more stable than the imine form in water. The formation of tautomers in the present experimental conditions can, therefore, be excluded and any aggregation of the monomer only involves the keto form (vide infra).

Photoluminescence of CZA Monomers and Dimers.

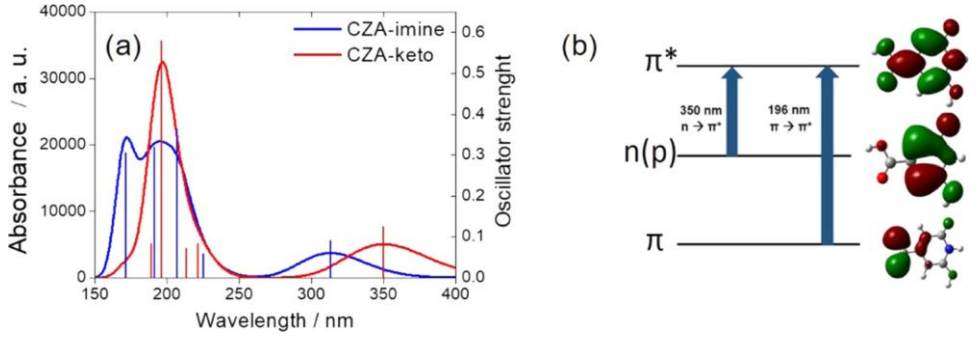

Figure 4. (a) Calculated UV−vis spectra of imine and keto monomers (b) HOMO−LUMO representation for CZA keto monomer. The molecular orbitals were plotted taking into account the transitions with higher oscillator strength for each absorption band.

Figure 4a shows the simulated absorption spectra of the monomeric species. The computed absorption spectrum of keto monomer is in good agreement with experimental data and shows two maxima at 197 and 350 nm, corresponding to $\pi \rightarrow \pi^*$ and $n \rightarrow \pi^*$ transitions. The corresponding highest occupied molecular orbital and lowest unoccupied molecular orbital (HOMO and LUMO, respectively) are reported in Figure 4b. The theoretical calculations, combined with the The concentration of CZA in water has been correlated with the photoemission properties through 3D fluorescence maps (excitation (y)−emission (x)−intensity (false color scale)) (Figure 5). CZA is fluorescent in the monomeric state with an emission in the blue range peaking at 440 nm. The 3D pattern is highly symmetrical indicating that the emission is only due to one specie: the monomer, in accordance with the UV−vis

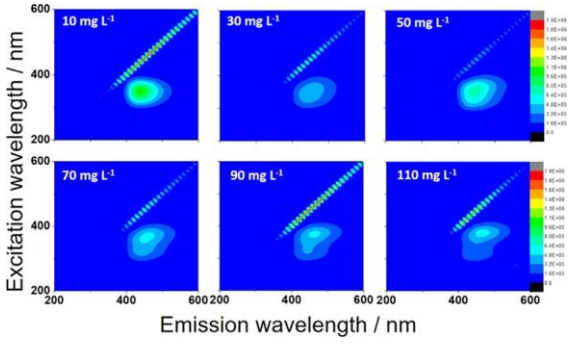

Figure 5. 3D fluorescence spectra (excitation−emission−intensity) of CZA in water at different concentrations from 10 up to 110 mg L^{-1}. The intensity is shown in a false color scale.

spectra. At higher concentrations, the emission mark loses the symmetry because other emissive species form. The 3D fluorescence maps show that the emission changes as a function of the CZA concentration and is coherent with the presence of two fluorescent species. Increasing the CZA concentration causes a decrease in the monomer emission intensity, which is due to the formation of less efficient dimeric species. One emission is attributed to the CZA monomers and the other one to the J-dimers. Monomers and dimers coexist at concentrations higher than 10 mg L^{-1}.

One way to discriminate the contribution of the two chemical species is to properly choose the excitation wavelength to maximize one component over the other one. Figure 6 shows the emission spectra of CZA as a function of concentration at different excitation wavelengths. Under constant excitation of 310 nm, the photoluminescence (PL) spectra reveal the presence of a band with a maximum at 440 nm (Figure 6a). The maximum appears concentrationindependent and retains its energy value. Therefore, the spectra are mainly caused by the contribution of monomeric species. However, it is worth to underline the broadening of spectral response toward higher wavelengths, proving the appearance of emitting dimers with the increase in concentration. Figure 6b shows the emissions of the different CZA solutions under irradiation at the maximum of excitation spectra (PLE). Since the maximum is concentration-dependent, PL spectra turn out to be characterized by the contribution of monomers and dimers at the same time, with a progressive red shift of the overall emission and the increase of dimer contribution.

Figure 7 shows the excitation spectra at the emission maxima. The fluorophore exhibits two excitation maxima with

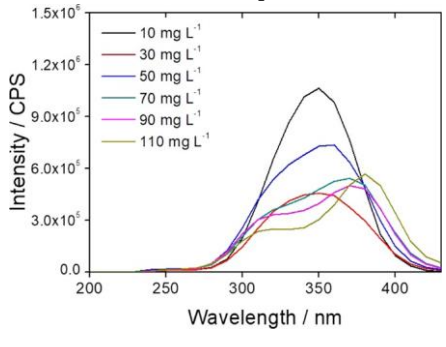

Figure 7. Excitation curves of CZA as a function of concentration. The spectra have been collected at the emission maxima.

the increase of CZA concentration, one at around 330−340 nm and the second one at 370 nm. These excitations are well in agreement with the two components obtained by the deconvolution of the absorption curves, testifying that the spectral trend in absorption is ascribable to the presence of two emitting species. At 10 mg L^{-1}, the fluorescence is dominated by one component, the CZA monomer. As soon as the dimers form, the shape of the CZA in the emission in the 3D map changes. At higher concentrations, the emission is given by two main components, one with excitation maxima at around 370 nm and another one at around 330 nm. The 330 nm band is mainly due to the emission of monomers and the other component due to the dimers.

There are two possible types of dimers that could form: sandwich H-dimers with intermolecular hydrogen bonding and π−π stacking of the pyridone unit and head-to-tail J-dimers (Scheme 2).[19,20]

Very little is known about the basic properties of citrazinic acid in water. The few references in the literature are correlated to processes where CZA and its derivatives are by-products synthesized employing citric acid and urea as precursors. These molecules are efficient fluorophores in the blue range. It has been reported that under a treatment at high temperature, CZA molecules can form aggregates by aromatic ring stacking.[21,22] In addition, the possibility of formation of dimers and tetramers of J-type has been also hypothesized. The relative calculations have produced contradictory results, in which J-dimers show a blue shift in the UV absorption spectra with respect to the monomer. A red shift is only obtained by invoking a tetrameric structure. Moreover, the two tautomers of citrazinic acid (imine and keto forms) are both involved in the dimerization process.[23–28]

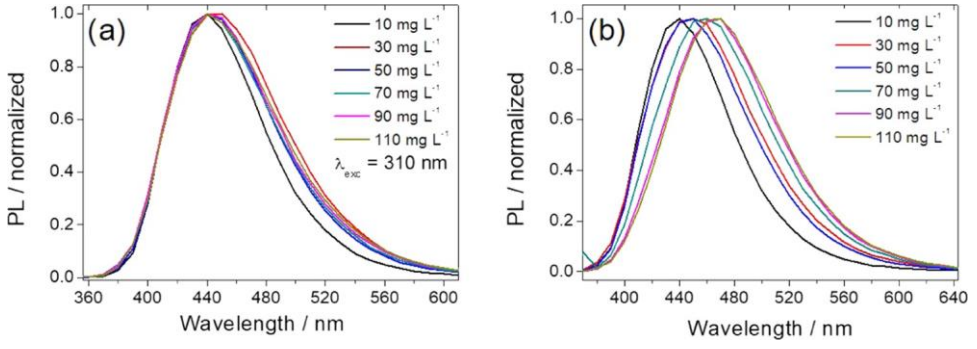

Figure 6. Emission dependence of CZA PL spectra. (a) PL spectra acquired under λ_{exc} = 310 nm. (b) PL spectra acquired at the maximum of PLE.

Scheme 2. Dimer Structures of Citrazinic Acid in J- and H-Type Configurations (a and b, Respectively)

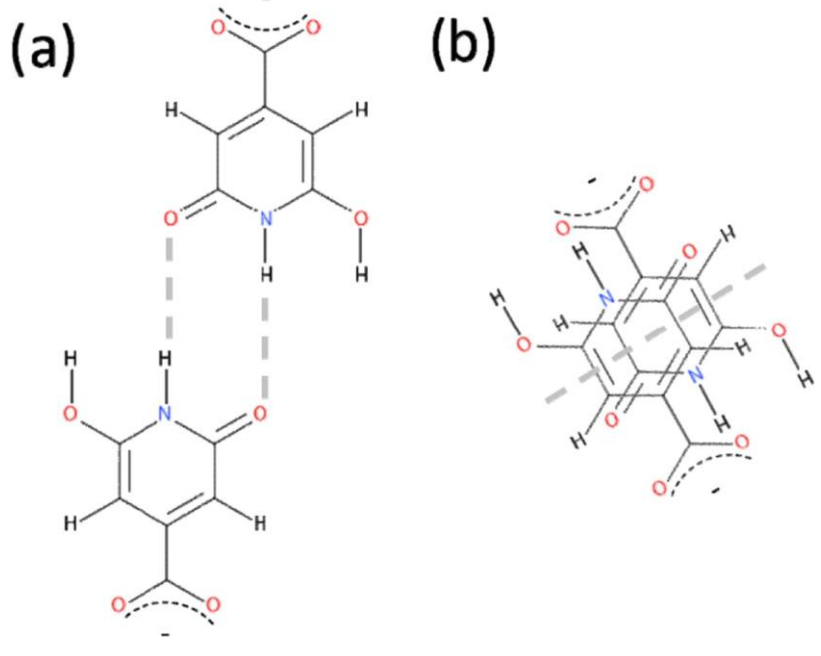

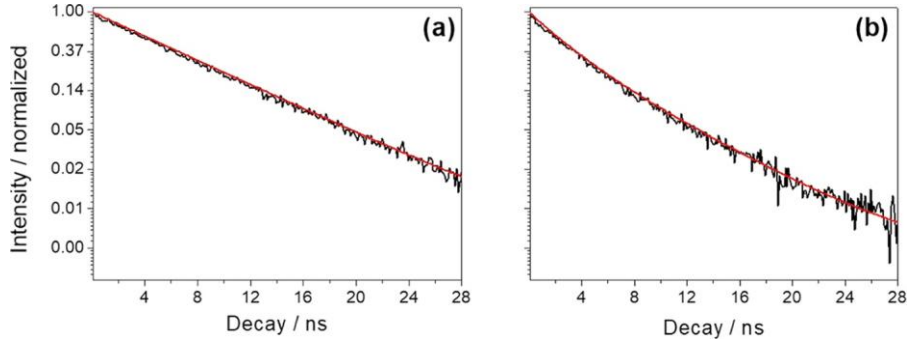

Figure 8. (a) Luminescence decay profile of the 10 mg L^{-1} citrazinic acid aqueous solution and (b) 110 mg L^{-1} (λ_{ex} = 340 nm).

Our computational calculations show the greater stability of the keto form compared to imine and a better agreement with the experimental absorption spectra. The CZA absorption spectra show only two bands, as previously underlined, the monomer and another one at higher wavelengths that we assign to dimers. We can suppose the formation of J-dimers through hydrogen bonds between the respective 6-hydroxy-2pyridone units in the form of N−H···O = R and R = O···O−H. This dimer is known to cause a red shift of the absorption spectra.[20] On the other hand, the presence of H-type dimers can be ruled out as they should exhibit an absorption band at lower wavelengths with respect to the monomer.

Another piece of experimental evidence of the presence of two emitting species is given by the time-resolved fluorescence analysis. Figure 8a shows the luminescence decay profile of the CZA solution in water at the concentration of 10 mg L^{-1}. At high dilution, with a wavelength at 340 nm, close to the maximum excitation (~350 nm), the fluorescence time decay shows a single exponential ($I = A \exp(-t/\tau)$) behavior, with a lifetime τ = 6.45 ns (Table 1). This is in accordance with the absorption spectra, where the nature of the single monomer allows fitting the experimental results by a single Gaussian band peaked at 344 nm. At low concentrations, the emission of Table 1. Lifetime of Low- and High-Concentrated CZA in Water

sample	λ_{exc}/nm	λ_{em}/nm	τ_1/ns	τ_2/ns	A_1	A_2
10 mg L^{-1}	340	440		6.45		1.00
110 mg L^{-1}	340	470	0.24	5.49	0.04	0.96

CZA is therefore dominated by the presence of monomers, whose optical recombinations have only one lifetime.

Higher concentration solutions (>10 mg L^{-1}) exhibit two characteristic PLE bands at 320 and 380 nm, respectively. The two maxima originate from the splitting of the band measured at low concentrations and can be traced back to the presence of two optically active chemical species, whose emissions overlap to form a wide band with a maximum at about 465 nm. The presence of the two excitation maxima suggests the possibility to selectively excite the two chemical species to reveal their respective contributions to the emission in the visible. Figure 8b shows the temporal decay of the luminescence of the samples at a concentration of 110 mg L^{-1}, with excitation at 340 nm. In this case, the luminescence decay does not present a single exponential decay.

Table 1 shows the best-fit parameters. By using doubleexponential law, the solution at 110 mg L^{-1} shows two lifetimes of 0.24 and 5.49 ns, attributed to the dimeric and the monomeric components, respectively. The contribution of the monomer is still predominant over the emission of the sample with the highest concentration (Table 1). At a high concentration (Figure 8b), the component with the longest lifetime (attributed to the emission of the monomer) is slightly shortened in the presence of dimers (from 6.45 to 5.49 ns). This effect is attributed to a nonradiative energy transfer from the monomeric to the dimeric species at a high concentration.[29,30]

Although the formation of larger aggregates, such as trimers and tetramers, cannot be ruled out, the identification of twodecay components suggests that one main aggregated specie is present and this is reasonably identified as a dimer.

Figure 9 shows the energy levels of CZA in water for the monomer and the dimer. CZA monomer shows well-defined

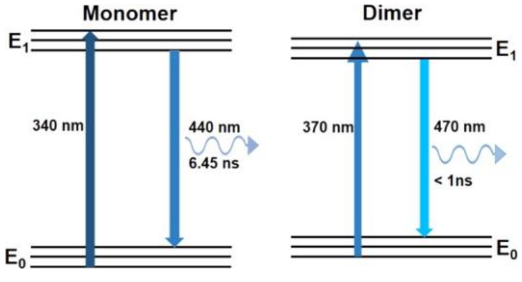

Figure 9. Energy levels of the proposed mechanism for CZA optical properties in water.

recombination in the blue region at 440 nm, corresponding to a single exponential decay. This behavior is only observed at a low concentration, where only monomeric species are present. In the presence of dimers (30−110 mg L^{-1}), an efficient component at a higher wavelength sums up to the monomeric one.

CONCLUSIONS

Understanding the mechanisms that govern the optical properties of citrazinic acid is very important to control the synthesis of the large family of carbon dots synthesized from citric acid and urea as precursors. In this article, we have investigated the optical properties of citrazinic acid in an aqueous environment over a wide concentration range. At low concentrations, citrazinic acid remains in the monomeric form with a characteristic emission in the blue range. The comparison of the theoretical and experimental results shows that in water there is only the keto tautomeric form of citrazinic acid. As the concentration increases, a new redshifted absorption band appears, which is assigned to J-type fluorescent dimers. The excitation spectra, with the rise of the aggregated form, show two overlapped bands. The lowest energy band is responsible for selective excitation of the aggregates. These aggregates have a shorter lifetime than the monomer and lower fluorescence efficiency. The optical response of citrazinic acid is, therefore, dependent on the formation of aggregates. They have to be carefully analyzed and controlled to modulate the emission of carbon dots where citrazinic acid and its derivatives can be formed during the synthesis process.

ASSOCIATED CONTENT

* Supporting Information

The Supporting Information is available free of charge at https://pubs.acs.org/doi/10.1021/acs.jpca.9b10884.

UV−vis spectra of CZA in water and EtOH; deconvolution curves in water; and SCF energy values (PDF)

AUTHOR INFORMATION

Corresponding Author

*E-mail: plinio@uniss.it.

ORCID

Luigi Stagi: 0000-0002-7238-8425

Luca Malfatti: 0000-0001-6901-8506

Carlo Maria Carbonaro: 0000-0001-6353-6409

Plinio Innocenzi: 0000-0003-2300-4680

Author Contributions

The manuscript was written through contributions of all authors. All authors have given approval to the final version of the manuscript.

Notes

The authors declare no competing financial interest.

ACKNOWLEDGMENTS

Italian Ministry of Education, University and Research (MIUR) is acknowledged for funding through the project PRIN 2017 n° 2017W75RAE. L.M. also acknowledges RAS for funding through the grant CRP 30, L.R. 7/2007 “Bando Capitale Umano ad Alta Qualificazione annualità 2015”.

REFERENCES

(1) Reckmeier, C. J.; Schneider, J.; Xiong, Y.; Hausler, J.; Kasäk, P.; Schnick, W.; Rogach, A. L. Aggregated Molecular Fluorophores in the Ammonothermal Synthesis of Carbon Dots. Chem. Mater. 2017, 29, 10352−10361.

(2) Ludmerczki, R.; Mura, S.; Carbonaro, C. M.; Mandity, I. M.; Carraro, M.; Senes, N.; Garroni, S.; Granozzi, G.; Calvillo, L.; Marras, S.; et al. Carbon Dots from Citric Acid and its Intermediates Formed by Thermal Decomposition. Chem. - Eur. J. 2019, 25, 11963−11974.

(3) Suzuki, K.; Malfatti, L.; Carboni, D.; Loche, D.; Casula, M.; Moretto, A.; Maggini, M.; Takahashi, M.; Innocenzi, P. Energy Transfer Induced by Carbon Quantum Dots in Porous Zinc Oxide Nanocomposite Films. J. Phys. Chem. C 2015, 119, 2837−2843. (4) Zhu, S.; Zhao, X.; Song, Y.; Lu, S.; Yang, B. Beyond Bottom-up Carbon Nanodots: Citric-Acid Derived Organic Molecules. Nano Today 2016, 11, 128−132.

(5) Suzuki, K.; Malfatti, L.; Takahashi, M.; Carboni, D.; Messina, F.; Tokudome, Y.; Takemoto, M.; Innocenzi, P. Design of Carbon Dots Photoluminescence through Organo-Functional Silane Grafting for Solid-State Emitting Devices. Sci. Rep. 2017, 7, No. 5469.

(6) Song, Y.; Zhu, S.; Zhang, S.; Fu, Y.; Wang, L.; Zhao, X.; Yang, B. Investigation from Chemical Structure to Photoluminescent Mechanism: A Type of Carbon Dots from the Pyrolysis of Citric acid and an Amine. J. Mater. Chem. C 2015, 3, 5976−5984. (7) Kasprzyk,

W.; Bednarz, S.; Zmudzki, P.; Galica, M.; Bogdal, D. Novel Efficient Fluorophores Synthesized from Citric Acid. RSC Adv. 2015, 5, 34795−34799.

(8) Vallan, L.; Urriolabeitia, E. P.; Ruiperez, F.; Matxain, J. M.; Canton-Vitoria, R.; Tagmatarchis, N.; Benito, A. M.; Maser, W. K. Supramolecular-Enhanced Charge Transfer within Entangled Polyamide Chains as the Origin of the Universal Blue Fluorescence of Polymer Carbon Dots. J. Am. Chem. Soc. 2018, 140, 12862−12869.

(9) Sell, W. J.; Easterfield, T. H. LXXIII.-Studies on Citrazinic Acid. Part I. J. Chem. Soc., Trans. 1893, 63, 1035−1051.

(10) Easterfield, T. H.; Sell, W. J. V. -Studies on Citrazinic Acid. Part II. J. Chem. Soc., Trans. 1894, 65, 28−31.

(11) Song, Y.; Zhu, S.; Zhang, S.; Fu, Y.; Wang, L.; Zhao, X.; Yang, B. Investigation from Chemical Structure to Photoluminescent Mechanism: A Type of Carbon Dots from the Pyrolysis of Citric Acid and an Amine. J. Mater. Chem. C 2015, 3, 5976−5984.

(12) Frisch, M. J.; Trucks, G. W.; Schlegel, H. B.; Scuseria, G. E.; Robb, M. A.; Cheeseman, J. R.; Scalmani, G.; Barone, V.; Petersson, G. A.; Nakatsuji, H. et al. Gaussian 16, revision C.01; Gaussian, Inc.:
Wallingford CT, 2016.

(13) Jiang, J.; Ou-yang, L.; Zhu, L.; Zheng, A.; Zou, J.; Yi, X.; Tang, H. Dependence of Electronic Structure of g-C3N4 on the Layer Number of its Nanosheets: A Study by Raman Spectroscopy Coupled with First-principles Calculations. Carbon 2014, 80, 213−221.

(14) Becke, A. D. Density-functional Thermochemistry. III. The Role of Exact Exchange. J. Chem. Phys. 1993, 98, 5648−5652.

(15) Lee, C.; Yang, W.; Parr, R. G. Development of the Colle-
Salvetti Correlation-energy Formula into a Functional of the Electron Density. Phys. Rev. B 1988, 37, 785−789.

(16) Klamt, A.; Moya, C.; Palomar, J. A Comprehensive Comparison of the IEFPCM and SS(V)PE Continuum Solvation Methods with the COSMO Approach. J. Chem. Theory Comput. 2015, 11, 4220−
4225.

(17) Dennington, R.; Keith, T. A.; Millam, J. M. GaussView, version 6; Semichem Inc.: Shawnee Mission, KS, 2016.

(18) Forlani, L.; Cristoni, G.; Boga, C.; Todesco, P. E.; Del Vecchio, E.; Selva, S.; Monari, M. Reinvestigation of the Tautomerism of Some Substituted 2-hydroxypyridines. Arkivoc 2002, 11, 198−215.

(19) Malfatti, L.; Kidchob, T.; Aiello, D.; Aiello, R.; Testa, F.; Innocenzi, P. Aggregation States of Rhodamine 6G in Mesostructured Silica Films. J. Phys. Chem. C 2008, 112, 16225−16230. (20) Lasio, B.; Malfatti, L.; Innocenzi, P. Photodegradation of Rhodamine 6G Dimers in Silica Sol-gel Films. J. Photochem. Photobiol., A 2013, 271, 93−98.

(21) Schneider, J.; Reckmeier, C. J.; Xiong, Y.; von Seckendorff, M.; Susha, A. S.; Kasa′k, P.; Rogach, A. L. Molecular Fluorescence in Citric Acid-Based Carbon Dots. J. Phys. Chem. C 2017, 121, 2014−
2022.

(22) Sarkar, S.; Chowdhury, J.; Dutta, S.; Pal, T. A pH Dependent Raman and Surface Enhanced Raman Spectroscopic Studies of Citrazinic Acid Aided by Theoretical Calculations. Spectrochim. Acta, Part A 2016, 169108−169115.

(23) Nandy, A.; Kumar, A.; Dwivedi, S.; Pal, S. K.; Panda, D. Connecting the Dots of Carbon Nanodots: Excitation (In)dependency and White-Light Emission in One-Step. J. Phys. Chem. C 2019, 123, 20502−20511.

(24) Szyc, Ł.; Guo, J.; Yang, M.; Dreyer, J.; Tolstoy, P. M.;
Nibbering, E. T. J.; Czarnik-Matusewicz, B.; Elsaesser, T.; Limbach, H.-H. The Hydrogen-Bonded 2-Pyridone Dimer Model System. Combined NMR and FT-IR Spectroscopy Study. J. Phys. Chem. A 2010, 114, 7749−7760.

(25) Khouri, S. J. Titrimetric Study of the Solubility and Dissociation of Benzoic Acid in Water: Effect of Ionic Strength and Temperature. Am. J. Anal. Chem. 2015, 6, 429−436.

(26) Hejazi, S. A.; Osman, O. I.; Alyoubi, A. O.; Aziz, S. G.; Hilal, R. H. The Thermodynamic and Kinetic Properties of 2-Hydroxypyridine/2-Pyridone Tautomerization: A Theoretical and Computational Revisit. Int. J. Mol. Sci. 2016, 17, 1893−1910.

(27) Frank, J.; Katritzky, A. R. Tautomeric Pyridines in Solvents of Differing Polarity Part XV. Pyridone-Hydroxypyridine EquiIibria. J. Chem. Soc. B 1968, 556−561.

(28) Aggarwal, N.; Patnaik, A. Dimeric Conformation Sensitive Electronic Excited States of Tetracene Congeners and their Unconventional Non-Fluorescent Behavior. J. Chem. Sci. 2019, 131, 52−66.

(29) Luridiana, A.; Pretta, G.; Chiriu, D.; Carbonaro, C. M.; Corpino, R.; Secci, F.; Frongia, A.; Stagi, L.; Ricci, P. C. A Facile Strategy for New Organic White LED Hybrid Devices: Design, Features and Engineering. RSC Adv. 2016, 6, 22111−22120.

(30) Stagi, L.; Chiriu, D.; Carbonaro, C. M.; Corpino, R.; Ricci, P.
C. Structural and Optical Properties of Carbon Nitride Polymorphs. Diamond Relat. Mater. 2016, 68, 84−92.